Applied and Environmental Microbiology, Oct. 2011, p. 6808–6820 Vol. 77, No. 19
0099-2240/11/$12.00 doi:10.1128/AEM.00219-11

Influence of Pore Structure on the Effectiveness of a Biogenic Carbonate Surface Treatment for Limestone Conservation▽

Willem De Muynck,[1,2] Stijn Leuridan,[1] Denis Van Loo,[3,4] Kim Verbeken,[5] Veerle Cnudde,[6] Nele De Belie,[1]* and Willy Verstraete[2]

Magnel Laboratory for Concrete Research, Department of Structural Engineering, Ghent University, Technologiepark Zwijnaarde 904, 9052 Ghent, Belgium[1]; Laboratory for Microbial Ecology and Technology (LabMET), Department of Biochemical and Microbial Technology, Ghent University, Coupure Links 653, 9000 Ghent, Belgium[2]; Department of Soil Management, Ghent University, Coupure Links 653, 9000 Ghent, Belgium[3]; Center for X-Ray Tomography (UGCT), Department of Physics and Astronomy, Ghent University, Proeftuinstraat 86, 9000 Ghent, Belgium[4]; Department of Materials Science and Engineering, Ghent University, Technologiepark Zwijnaarde 903, 9052 Ghent, Belgium[5]; and Department of Geology and Soil Science, Ghent University, Krijgslaan 281, S8, 9000 Ghent, Belgium[6]

Received 1 February 2011/Accepted 28 July 2011

A ureolytic biodeposition treatment was applied to five types of limestone in order to investigate the effect of pore structure on the protective performance of a biogenic carbonate surface treatment. Protective performance was assessed by means of transport and degradation processes, and the penetration depth of the treatment was visualized by microtomography. Pore size governs bacterial adsorption and hence the location and amount of carbonate precipitated. This study indicated that in macroporous stone, biogenic carbonate formation occurred to a larger extent and at greater depths than in microporous stone. As a consequence, the biodeposition treatment exhibited the greatest protective performance on macroporous stone. While precipitation was limited to the outer surface of microporous stone, biogenic carbonate formation occurred at depths of greater than 2 mm for Savonnières and Euville. For Savonnières, the presence of biogenic carbonate resulted in a 20-fold decreased rate of water absorption, which resulted in increased resistance to sodium sulfate attack and to freezing and thawing. While untreated samples were completely degraded after 15 cycles of salt attack, no damage was observed in biodeposition-treated Savonnières. From this study, it is clear that biodeposition is very effective and more feasible for macroporous stones than for microporous stones.

The evidence of microbial involvement in carbonate precipitation has led to the exploration of this process in a variety of fields, including environmental, civil, and geological engineering (7). Among these applications, microbiologically induced carbonate precipitation (MICP) has been used for the production of a biogenic-carbonate-based surface treatment, a process known as biodeposition (1, 10, 20, 21). Since the discovery that MICP can be applied for the protection of stone (1), several researchers have tried to optimize its performance (7). Initial studies were focused mainly on the microbiological aspects of MICP, i.e., the type of microorganism and the metabolic pathway. Several metabolic pathways affect the factors that govern calcium carbonate precipitation, including (i) the concentration of dissolved inorganic carbon, (ii) the pH, and (iii) the concentration of calcium ions (3, 13). Furthermore, the physical and chemical characteristics of the bacterial cells can make them act as sites of crystal nucleation, which is another important factor in carbonate precipitation (13).

In a first attempt to improve the effectiveness of the biodeposition treatment, previous studies by our research group were focused on the ureolytic pathway (6, 8, 10, 12). Contrary to other metabolic pathways, the hydrolysis of urea can be easily controlled and allows the production of high concentrations of carbonate within a short period of time (minutes to hours), making it a very feasible pathway for biodeposition applications in practice (7).

In an effort to further improve the effectiveness of the ureolytic biodeposition treatment, we have recently investigated the influence of the chemical aspects of biogenic calcium carbonate precipitation, i.e., the dosage of urea and calcium (9). From that study, an optimum dosage of urea and calcium was found; additionally, it was determined that dosing above said limit induces more detrimental effects (i.e., accumulation of salts and discoloration of the stone) than benefits (i.e., additional precipitation of carbonate and hence an increased protective effect) (9).

From the above statements, it is clear that studies regarding the parameters that influence the effectiveness of the biodeposition treatment were related mainly to the microbiological and chemical aspects of the biogenic carbonate surface treatment. However, one of the most important parameters affecting the performance of a surface treatment, i.e., penetration depth, remained largely overlooked. So far, in many studies of biodeposition, the distribution of biogenic crystals was evaluated only by microscopic investigation of the outer surface. In such experiments, Zamarreño et al. (32) observed that biogenic crystals were preferentially formed around and inside open pore spaces. Their biodeposition treatment resulted in a decrease in pore size of about 50% without blocking the pores

* Corresponding author. Mailing address: Laboratory for Microbial Ecology and Technology (LabMET), Department of Biochemical and Microbial Technology, Ghent University, Coupure Links 653, 9000 Ghent, Belgium. Phone: 32 9 264 55 22. Fax: 32 9 264 58 45. E-mail: nele.debelie@ugent.be.

▽ Published ahead of print on 5 August 2011.

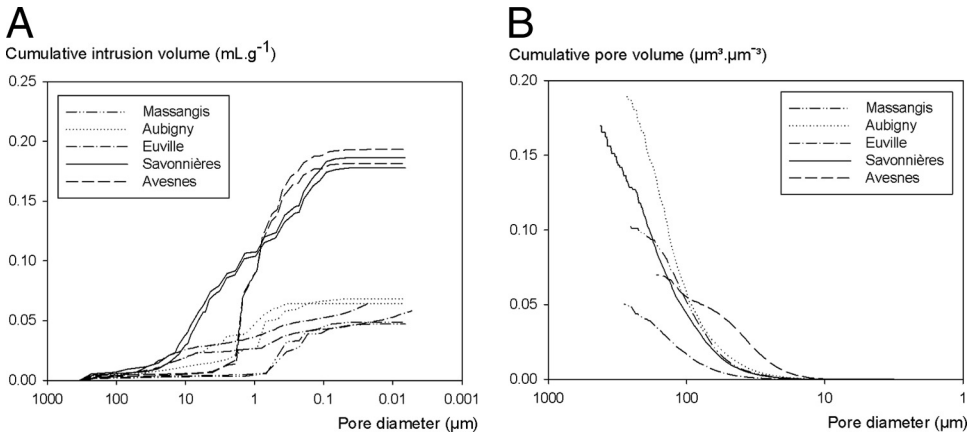

FIG. 1. Pore size distributions of the different types of limestone used in this study as determined by MIP (A) and microtomography (B).

completely, and from this information, the authors concluded their treatment to be safe for conservation purposes. Only a few studies, however, have reported on the distribution of biogenic crystals throughout the stone. From scanning electron microscopy (SEM) analyses of cross sections of biodeposition-treated stone, precipitation has been observed at depths of about 100 μm for the Calcite Bioconcept treatment (7). Rodriguez-Navarro et al. (21) observed precipitation at depths of greater than 500 μm in a macroporous bioclastic calcarenite. However, those studies did not elaborate on the relationship that exists between the penetration depth and the performance of the biodeposition treatment. Torraca indicated that a consolidant should be able to penetrate stone to such a depth that all loose material is consolidated and attached to the intact core of the stone (25). From the findings described above, it appears that the consolidative effect of many biodeposition procedures will be rather limited in depth; in order to further improve the performance of the biodeposition treatment, it is necessary to gain a better understanding of the parameters that affect the penetration depth of the biodeposition treatment.

For all types of surface treatments, the depth of penetration depends on a variety of parameters; in addition to climatologic conditions, it is influenced by viscosity, surface tension, rate of deposition, application procedure, and rate of solvent evaporation (4). Moreover, since liquid transport is dependent on the pore structure of a stone (porosity, pore shape, and pore connectivity), the latter will also affect the penetration depth of a surface treatment. For the biodeposition treatments, the depth of penetration depends not only on the transport of liquid through the stone but also on that of the bacteria. Transport of bacteria through a porous material depends both on the pore structure of the stone and the adsorption of the bacteria to the mineral matrix. Transport of bacteria occurs in pores the diameter of which is about two times that of the bacteria (26). Adsorption of bacteria, on the other hand, is governed by a variety of physical, chemical, and microbiological factors (24). Physical factors relate to the porous medium (specific surface, surface roughness, and electrostatic charges), temperature, and rate of water transport. Ionic strength and pH are examples of chemical factors and microbiological factors relate to hydrophobicity, chemotaxis, and cell surface charges.

The aim of this study was to investigate how pore structure influences the penetration depth and, more generally, the performance of a biodeposition treatment (i.e., consolidative effect and protection against the ingress of water and chemicals). The outcome of this paper could then be used to select stone types on which the biodeposition treatment has the greatest effect. To our knowledge, this is the first paper in which the performance of the biodeposition treatment on different types of stone is reported.

MATERIALS AND METHODS

Microorganisms. Biodeposition experiments were performed with *Bacillus sphaericus* LMG 22257 (Belgian Coordinated Collections of Microorganisms, Ghent, Belgium). The selection of this spore-forming strain was based upon earlier work (10, 11). The liquid culture medium used consisted of 20 g liter^{-1} yeast extract and 20 g liter^{-1} urea (VWR International) and was sterilized by autoclaving for 20 min at 120°C. Urea was added after autoclaving by filtration through a sterile 0.22-μm Millipore filter. For all experiments, *B. sphaericus* cultures were obtained after subsequent culturing (two times and 1% inoculum) from a −80°C stock culture. Cultures were incubated for 24 h at 28°C on a shaker at 100 rpm. Culturing was performed under sterile conditions.

Stones. Experiments were performed on five types of French limestone, including Massangis, Euville, Aubigny, Savonnières, and Avesnes. Selection of stones was directed by availability and (historical) use in the Belgian cultural heritage. Furthermore, care was taken to obtain stones with different types of pore structure (Fig. 1). The stones were provided by a Belgian restoration company. Aubigny is an oolithic limestone. Savonnières (Late Thinothian, Upper Jura) is an oolithic limestone with a sparry calcite cement which contains 98 to 99% calcium carbonate and consists of bioclasts and ooliths with dissolved nuclei. Massangis Roche Jaune (Bathonian, Middle Jura) is an oolithic limestone composed mostly of calcium carbonate, but dolomite and iron oxide can be present. The nuclei of the ooliths are not dissolved, unlike those of Savonnières. Besides oolithic fragments, bioclasts can also be found, together with a fine-grained micritic cement. Euville (Oxfordian, Upper Jura) is a crinoidal limestone which consists of around 98% calcium carbonate and contains a large number of crinoid fragments which are cemented by a microcrystalline mass. The Avesnes limestone (Turonian, Upper Cretaceous) typically contains small amounts of glauconite, detritic quartz, bioclasts, and opaque minerals in a micrite cement. This stone can be classified as a bioclastic wackestone. For biodeposition experiments, stone blocks were cut into specimens with different dimensions, i.e., prisms of 40 mm by 20 mm by 10 mm, cubes with 40-mm sides, and cylinders 4 to 5 mm in diameter and 4 to 8 mm in height. Prior to all experiments, specimens were stored in an oven at 80°C until a constant weight was attained (a weight change of less than 0.1% between two measurements at 24-h intervals) was achieved.

Biodeposition treatment procedure. Biodeposition treatment was performed in an incubation room at 28°C under static and nonsterile (open to the air) conditions. In the first step, stone specimens were immersed for 24 h in a 1-day-old culture of *B. sphaericus* (pH 9.45, Table 1). After this incubation

TABLE 1. Weight gain of limestone prisms for different types of biodeposition treatments

Stone type (mean % porosity ± SEM) and treatment	pH[a]				Weight gain	
	Step 1		Step 2			
	Initial	Final	Initial	Final	Absolute (g, %)[b]	Relative (%, %)[b]
Less porous						
Massangis (9.98 ± 0.66)						
Medium	6.89	7.73	7.41	6.81	0.07 ± 0.01 (27)	0.37 ± 0.04 (25)
Bacteria in saline	6.65	7.8	NA[d]	NA	0.00 ± 0.00 (0)	0.00 ± 0.00 (0)
Bacteria in culture liquid	9.45	7.89	NA	NA	0.03 ± 0.00 (12)	0.16 ± 0.02 (11)
Biodeposition with supernatant	9.42	9.04	7.41	6.86	0.09 ± 0.02 (34)	0.46 ± 0.09 (31)
Biodeposition with bacteria in saline	6.65	7.8	NA	5.5	0.22 ± 0.03 (83)	1.11 ± 0.13 (74)
Biodeposition with bacteria in culture liquid	9.43	ND[c]	ND	ND	0.27 ± 0.01	1.49 ± 0.04
Aubigny (14.12 ± 0.34)						
Medium	6.89	7.72	7.41	6.77	0.12 ± 0.01 (22)	0.71 ± 0.07 (24)
Bacteria in saline	6.65	7.85	NA	NA	0.00 ± 0.00 (1)	0.02 ± 0.01 (1)
Bacteria in culture liquid	9.45	7.11	NA	NA	0.06 ± 0.01 (11)	0.38 ± 0.05 (13)
Biodeposition with supernatant	9.42	8.74	7.41	6.73	0.21 ± 0.03 (38)	1.29 ± 0.16 (43)
Biodeposition with bacteria in saline	6.65	7.85	NA	5.54	0.39 ± 0.03 (71)	2.18 ± 0.18 (72)
Biodeposition with bacteria in culture liquid	9.43	ND	NA	ND	0.55 ± 0.02	3.02 ± 0.13
Euville (17.24 ± 0.59)						
Medium	6.89	7.69	7.41	7.52	0.11 ± 0.02 (16)	0.67 ± 0.14 (20)
Bacteria in saline	6.65	7.85	NA	NA	0.00 ± 0.01 (0)	0.00 ± 0.03 (0)
Bacteria in culture liquid	9.45	7.58	NA	NA	0.05 ± 0.01 (8)	0.33 ± 0.05 (10)
Biodeposition with supernatant	9.42	8.99	7.41	6.98	0.17 ± 0.02 (26)	1.03 ± 0.10 (30)
Biodeposition with bacteria in saline	6.65	7.85	7.41	5.8	0.39 ± 0.04 (61)	2.15 ± 0.24 (63)
Biodeposition with bacteria in culture liquid	9.43	ND	ND	ND	0.64 ± 0.08	3.40 ± 0.29
More porous						
Savonnières (30.92 ± 0.14)						
Medium	6.89	7.6	7.41	6.79	0.20 ± 0.03 (30)	1.48 ± 0.20 (33)
Bacteria in saline	6.65	7.8	NA	NA	0.00 ± 0.00 (0)	0.00 ± 0.03 (0)
Bacteria in culture liquid	9.45	7.65	NA	NA	0.08 ± 0.01 (13)	0.63 ± 0.12 (14)
Biodeposition with supernatant	9.42	9.11	7.41	6.93	0.20 ± 0.02 (31)	1.49 ± 0.13 (33)
Biodeposition with bacteria in saline	6.65	7.8	7.41	5.74	0.63 ± 0.05 (97)	4.73 ± 0.40 (105)
Biodeposition with bacteria in culture liquid	9.43	ND	NA	ND	0.65 ± 0.01	4.51 ± 0.05
Avesnes (32.10 ± 0.05)						
Medium	6.89	7.68	7.41	6.78	0.22 ± 0.01 (36)	1.74 ± 0.15 (40)
Bacteria in saline	6.65	7.65	NA	NA	−0.01 ± 0.00 (−1)	−0.07 ± 0.02 (−2)
Bacteria in culture liquid	9.45	7.97	NA	NA	0.10 ± 0.02 (16)	0.71 ± 0.08 (16)
Biodeposition with supernatant	9.42	8.97	7.41	6.63	0.31 ± 0.06 (51)	2.32 ± 0.25 (53)
Biodeposition with bacteria in saline	ND	ND	ND	ND	ND	ND
Biodeposition with bacteria in culture liquid	9.43	ND	ND	ND	0.61 ± 0.01	4.34 ± 0.05

[a] Columns 2 to 5 indicate the evolution of the pH during the different steps of the biodeposition treatment. Porosity was determined from water saturation under vacuum.
[b] Percent weight gain of prisms treated by biodeposition of bacteria in culture liquid. Values are means ± the standard errors of the means.
[c] ND, not determined.
[d] NA, not applicable.

period, specimens were removed from the culture solution (20 g liter^{-1} yeast extract and 20 g liter^{-1} urea) and gently wiped with a paper towel to remove excess liquid from the surface. In the second step, specimens were immersed for 4 days in a biodeposition medium containing 20 g liter^{-1} urea and 50 g liter^{-1} $CaCl_2 \cdot 2H_2O$. Among the different concentrations of urea and calcium tested, this composition appeared to be the best suited for biodeposition purposes (9). In both steps, the pH of the different liquids was measured before and after immersion of the prisms (Table 1). Depending on the durability parameter to be tested, specimens were treated either on one side (partial immersion) or on all sides (complete immersion). Cubes ($n = 4$) were completely immersed (for salt attack and freezing-and-thawing experiments) or immersed to a depth of about 1 cm (for water absorption and drying behavior experiments), while prisms ($n = 6$) were fully immersed in aluminum vessels containing 200 ml of biodeposition or culture medium. Cylinders for microtomographic analyses were treated together with the prisms (i.e., fully immersed in the same vessels at the same time). Next, the specimens were left to dry for 3 days at 28°C before they were stored in an oven at 80°C until a constant weight was obtained.

Characterization of the stone. The pore structure of the different stones was studied using mercury intrusion porosimetry (MIP) with a Micromeritics AutoPore IV device. MIP analyses were performed on untreated prisms ($n = 2$) with dimensions of 10 mm by 20 mm by 10 mm. Additionally, the porosity of oven-dried 40-mm stone cubes ($n = 4$) was determined by saturation with water under vacuum.

Characterization of the ureolytic activity inside the stone. The ureolytic activity of the different stones was determined by conductivity measurements with a Consort C562 multimeter. Six prisms of each type of stone were completely immersed for 24 h in a 1-day-old culture of *B. sphaericus* (pH 9.45). Afterward, the prisms were gently wiped with a paper towel and stored separately in Erlenmeyer flasks containing 100 ml of a urea solution (20 g liter^{-1} urea and 8.5 g liter^{-1} NaCl). Experiments were performed under stationary and nonsterile conditions. At specific times, the conductivity and pH of the solution were measured. For that purpose, 2 ml of solution was transferred to plastic tubes into which pH and conductivity probes were inserted, which was done to prevent contamination of the original solutions. The amount of urea hydrolyzed was

determined from the change in conductivity by the following relationship (5): urea hydrolyzed (mM) = change in conductivity (mS cm^{-1}) × 9.6 (R^2 = 0.9895).

Additionally, in two separate experiments, the influence of the bacterial cell number on the rate of urea hydrolysis was determined both in the presence and in the absence of calcium. For that purpose, 1-day-old cultures of *B. sphaericus* were serially diluted in sterile saline (8.5 g $liter^{-1}$ NaCl). Before dilution, the culture was centrifuged (Sorvall RC5Cplus centrifuge, 7,000 × *g* for 7 min), washed, and concentrated 10 times in sterile saline. For each dilution (n = 3), 1 ml of solution was transferred to an Erlenmeyer flask containing 99 ml of a urea solution (20 g $liter^{-1}$ urea and 8.5 g $liter^{-1}$ NaCl) or a urea-calcium solution (30 g $liter^{-1}$ urea and 75 g $liter^{-1}$ $CaCl_2 \cdot 2H_2O$).

Characterization of the biodeposition layer. (i) Thin sections and SEM analysis. Fluorescent-epoxy-impregnated thin sections of the untreated and biodeposition-treated specimens were prepared as described by Jakobsen and Brown (15). For the treatments under investigation here, two thin sections (40 mm by 25 mm) were prepared from one specimen (a cube) (n = 2). Thin sections were analyzed with a Leica DMLP microscope (Leica Microsystems) connected to a Canon S50 camera.

Limestone samples (10-mm side chunks from treated and untreated prisms; n = 2) for SEM analysis were coated with a thin gold layer with an SCD005 Sputter Coater (Bal-Tec AG, Principality of Liechtenstein). The samples were subsequently studied with an FEI XL30 scanning electron microscope equipped with a LaB6 filament and with an energy-dispersive X-ray spectroscopy (EDX) detector (EDAX).

(ii) Microtomographic analyses. For microtomographic analyses, cylinders (4 to 5 mm in diameter and 4 to 8 mm in height; n = 1) were scanned prior to and after biodeposition treatment using the multiresolution X-ray tomography setup at the Ghent University Center for X-Ray Tomography. This setup consists of a directional target X-ray tube and a flat-panel detector (http://www.ugct.ugent.be/instruments.php). With a tube voltage of 100 kV and an exposure time of 2 s per projection, 1,400 projections were recorded over a rotation of 360°. The raw data were reconstructed using the reconstruction software Octopus (developed in-house; 28), which resulted in a data set of 1,500 by 1,500 by 1,800 isotropic voxels (volumetric picture elements) with a voxel pitch of 4 μm.

Two data sets (pre- and posttreatment) per core were loaded into the rendering software Volume Graphics, and the data sets were realigned with the same positioning and orientation in three-dimensional (3D) space. The rock volume of the pretreatment sample was thresholded based on gray values and subtracted from the rock volume of the posttreatment data set; the resulting rock volume was colored yellow and can be considered the effect of the treatment. In order to compensate for small misalignments and partial volume effects (i.e., in order to prevent an overestimation of the amount of newly formed carbonates), the thresholded pretreatment volume was expanded by one pixel in all directions prior to subtraction from the posttreatment volume. For the 3D visualization, a rectangular region was extracted from the yellow volume and separately displayed in order to get an appreciation of the internal structure. The penetration depth of the treatment was determined by image analysis of 2D slices; ImageJ (http://rsb.info.nih.gov/ij/ ed) was used for that purpose. For the determination of pore size distribution, the reconstructed data were processed with Morpho+ (a software program developed in-house) using a sequence of thresholding, separation, and distribution into intervals. Thresholding was performed based on gray values in order to separate stone from pores, the watershed algorithm was used for separation, and the distribution was based on the equivalent diameter of the pore volume.

(iii) Weight increase. The amount of carbonate precipitated onto the specimens was estimated from the weight increase of the limestone prisms due to the biodeposition treatment (n = 6). The weight gain was calculated from the difference in weight before and after treatment, after drying in an oven at 80°C until a constant weight was attained (precision of balance, 0.1 mg). In order to evaluate the contribution of the biomass and abiotic carbonate precipitation to the overall weight increase, the following control series were included: bacteria (in culture liquid or in saline), medium, and supernatant. For the medium and supernatant series, the treatment procedure was similar to the biodeposition series, except for the first day, on which the limestone specimens were immersed for 24 h in medium (20 g $liter^{-1}$ urea and 20 g $liter^{-1}$ yeast extract) and supernatant, respectively. The supernatant was obtained after the centrifugation of a 1-day-old culture of *B. sphaericus* (Sorvall RC5Cplus centrifuge, 7,000 × *g* for 7 min). For the bacterium series, the limestone prisms remained immersed in the *B. sphaericus* culture (in culture liquid or in saline) for a period of 1 day, without being immersed in the biodeposition medium afterward.

(iv) Spectrophotometric analyses. The influence of the biodeposition treatment on the chromatic aspect of the stones was determined by spectrophotometric measurements; an X-Rite SP60 spectrophotometer with a circular measurement area 8 mm in diameter was used for that purpose. Reflectance measurements were recorded at four points distributed over the surface of each of the four limestone cubes used for the water absorption experiments, i.e., 16 measurements for each treatment (n = 16). Differences in visual aspect were expressed as the CIELab ΔE value, which is calculated as follows (2):

$$\Delta E = \sqrt{\Delta L^{*2} + \Delta a^{*2} + \Delta b^{*2}}$$

with Δ being the difference between the mean values of the treated cubes and the untreated reference series. The L^* values range from 0 to +100 and represent black and white, respectively; the negative and positive a^* values represent green and red, respectively; and the negative and positive b^* values represent blue and yellow, respectively.

Evaluation of the protective performance of the biodeposition treatment. (i) Capillary water absorption. Determination of water absorption by capillarity was performed with four cubes per treatment according to BS EN 1925:1999 (n = 4). The specimens were immersed in water for 1 week (~780 $s^{0.5}$) with the treated side downward. The four sides of the dry specimens adjacent to the treated side were coated with butyl tape in order to prevent the evaporation of water through the sides during the water absorption experiments. The water absorption rate coefficient, k (cm $s^{-1/2}$), was obtained by using the expression:

$$\frac{Q}{A} = k\sqrt{t}$$

where Q is the amount of water absorbed (cm^3), A is the cross section of the specimen that was in contact with water (cm^2), t is time (seconds), Q/A was plotted against the square root of t, and k was calculated from the slope of the linear relationship (first 4 measurements) between the former.

(ii) Drying behavior. The influence of the biodeposition treatment on the drying behavior of the stone was investigated with an open-air desorption test. Limestone cubes (n = 4) that had been subjected to capillary water absorption for 7 days (i.e., time after which water absorption was stable over 48 h and after which no differences were observed between the water absorption of untreated and treated specimens) were removed from the water and wiped with a wet towel. Subsequently, the side opposite the treated side was covered with butyl tape so that evaporation of water from the treated side only could occur. The specimens were stored in a climate-controlled room (20°C and 65% relative humidity) with the treated face upward, and at regular intervals, the weight loss of the specimens was determined.

(iii) Resistance to sonication. The adhesion of the newly formed carbonates to the limestone specimens and the consolidating effect of the biodeposition treatment were determined by sonication as proposed by Rodriguez-Navarro et al. (21). Untreated and biodeposition-treated prisms (n = 6) were subjected to six cycles of sonication; during each cycle, the specimens were immersed for 5 min in demineralized water in a 35-kHz ultrasonic bath (Haver VSC 200-76; 120 to 240 W; Haver & Boecker) and after each cycle, the samples were dried for 48 h in an oven at 80°C and subsequently weighed.

(iv) Resistance to salt attack. The influence of the biodeposition treatment on the resistance of stone to salt attack was determined as described by Karatasios et al. (17). Treated and untreated cubes (n = 4) were subjected to 20 cycles of salt attack; each cycle lasted 24 h. During the first 2 h, the cubes were immersed in a sodium sulfate solution (14 wt%, Na_2SO_4)-containing vessel covered with plastic foil to prevent evaporation. Subsequently, the specimens were dried at 70 ± 5°C for 22 h in an oven that contained a beaker with water to sustain a high relative humidity. Finally, the specimens were weighed and photographed with a CanonScan Lide 70 scanner.

(v) Resistance to freezing and thawing. The influence of the biodeposition treatment on the resistance of stone to freezing and thawing was determined according to Belgian standard NBN B05-203 (1977). Prior to the test, the porosity of the cubes (n = 4) was determined by water saturation under vacuum, where the stones remained saturated with water until they were subjected to 14 cycles of freezing and thawing; each cycle lasted 24 h (16 h of freezing and 8 h of thawing). Damage was evaluated visually.

(vi) Statistical analysis. Error bars on graphs and values in tables represent standard errors. Comparison of mean values was performed by one-way analysis of variance using the SPSS 12.0 statistical software (P = 0.05).

RESULTS

Characterization of the stones. The different types of stone under investigation exhibited large differences in pore size distribution and porosity, as shown in Fig. 1 and Table 1 (see

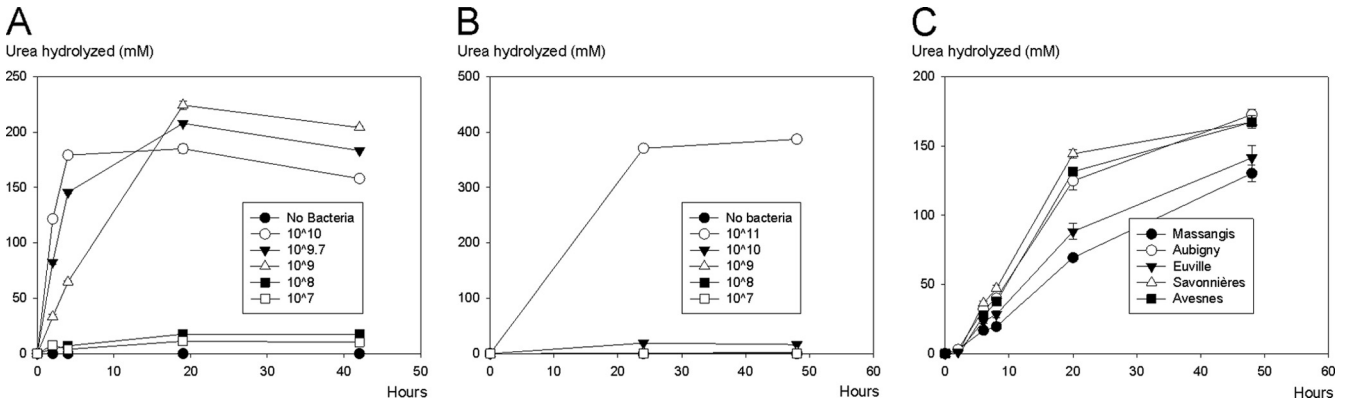

FIG. 2. Influences of the cell number (A), the presence of calcium (B), and the stone type (C) on the amount of urea hydrolyzed by *B. sphaericus* cultures.

also Fig. 5). The lowest porosity (ca. 10%), as determined by vacuum water absorption, was observed in Massangis (Table 1), while the highest porosity (ca. 30%) was observed in the Savonnières and Avesnes limestones. Aubigny and Euville had a porosity between the former two values (ca. 15%). The most porous stones, i.e., Savonnières and Avesnes, show clear differences in pore size distribution, as determined by MIP (Fig. 1A). Avesnes consisted mainly of pores between 0.1 and 1 μm, while Savonnières consisted mainly of pores between 0.5 and 10 μm. In Avesnes, pores larger than 5 μm in diameter are nearly absent. Similar observations were made for Massangis, in which pores larger than 1 μm were nearly absent. Although being similar in pore structure, Euville exhibited somewhat more micropores (0.01 to 0.1 μm) and macropores (10 to 100 μm) than Aubigny. From microtomographic analyses (Fig. 1B; see also Fig. 5), however, it is clear that MIP underestimated the amount of macropores, especially for stones such as Massangis, Aubigny, and Avesnes.

Characterization of the ureolytic activity of the stone. Limestone that had been immersed in *B. sphaericus* cultures exhibited ureolytic activity upon transfer to a urea-containing solution (Fig. 2). The rate of hydrolysis and the amount of urea hydrolyzed were observed to be dependent on the type of stone (Fig. 2C). The lowest rate was observed in Massangis limestone, followed by Euville limestone. Aubigny and Avesnes showed similar rates of urea hydrolysis. After 20 h, the largest amount of urea hydrolyzed was observed in Savonnières limestone. Figure 2A shows that the rate of hydrolysis also depended on the number of cells present in the solution. The fastest hydrolysis was observed in Erlenmeyer flasks in which 10^{10} cells were present (i.e., 100 ml of 10^8 cells ml^{-1}), and limited to no hydrolysis of urea was observed in Erlenmeyer flasks in which fewer than 10^9 cells were present (i.e., fewer than 10^7 cells ml^{-1}). In the presence of 75 g $liter^{-1}$ calcium chloride, significant hydrolysis of urea was observed only in Erlenmeyer flasks in which 10^{11} cells were present, and in those Erlenmeyer flasks, massive precipitation of calcium carbonate was observed.

Characterization of the biodeposition layer. (i) Thin-section, SEM, and microtomographic analyses. Biogenic carbonate crystals exhibited variations in both size (1 to 100 μm) and morphology (rhombohedra, spheres, etc.) (Fig. 3); these dif-

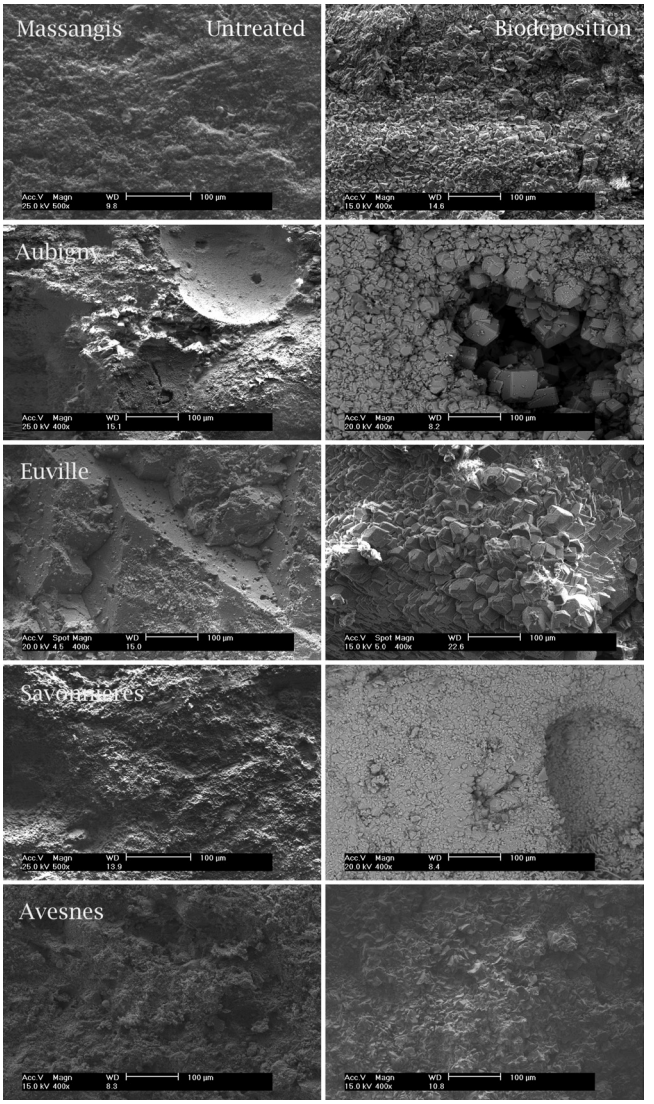

FIG. 3. Scanning electron micrographs (top view) of untreated (pictures on the left) and biodeposition-treated (pictures on the right) limestone. Note the presence of a newly formed layer of carbonate crystals on the surface of biodeposition-treated limestone.

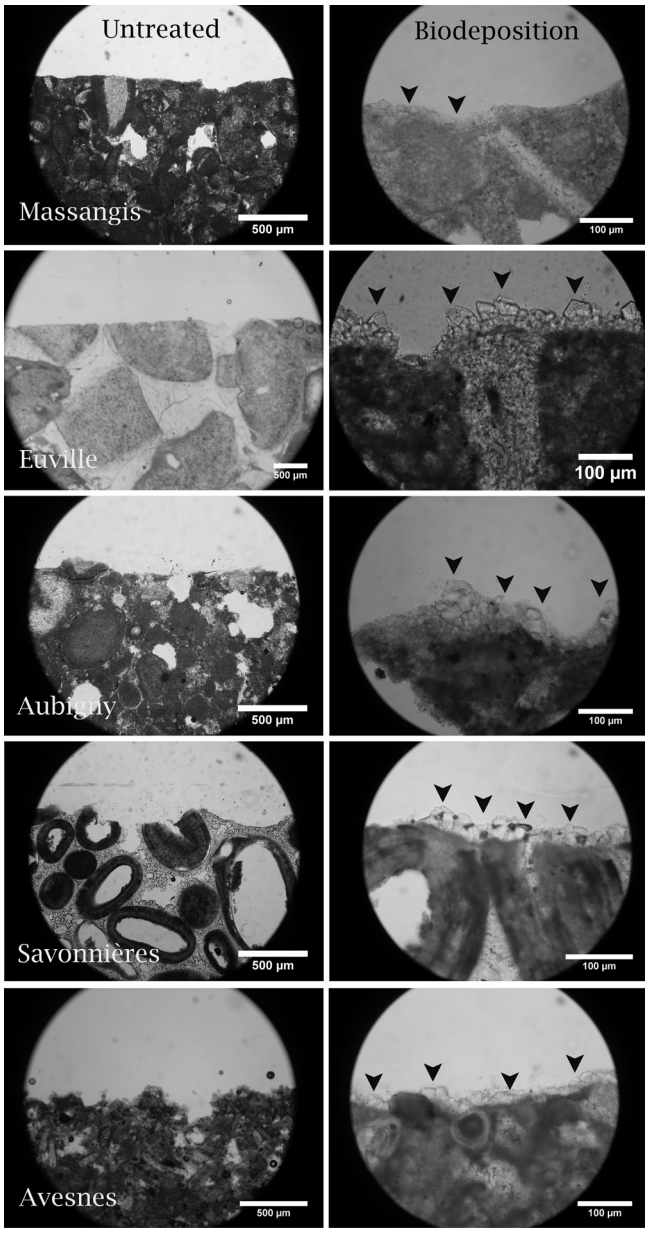

FIG. 4. Thin sections of untreated (pictures on the left) and biodeposition-treated (pictures on the right) limestone. Note the differences in the amounts and sizes of the newly formed carbonate crystals (indicated by black arrowheads) on different types of biodeposition-treated stone.

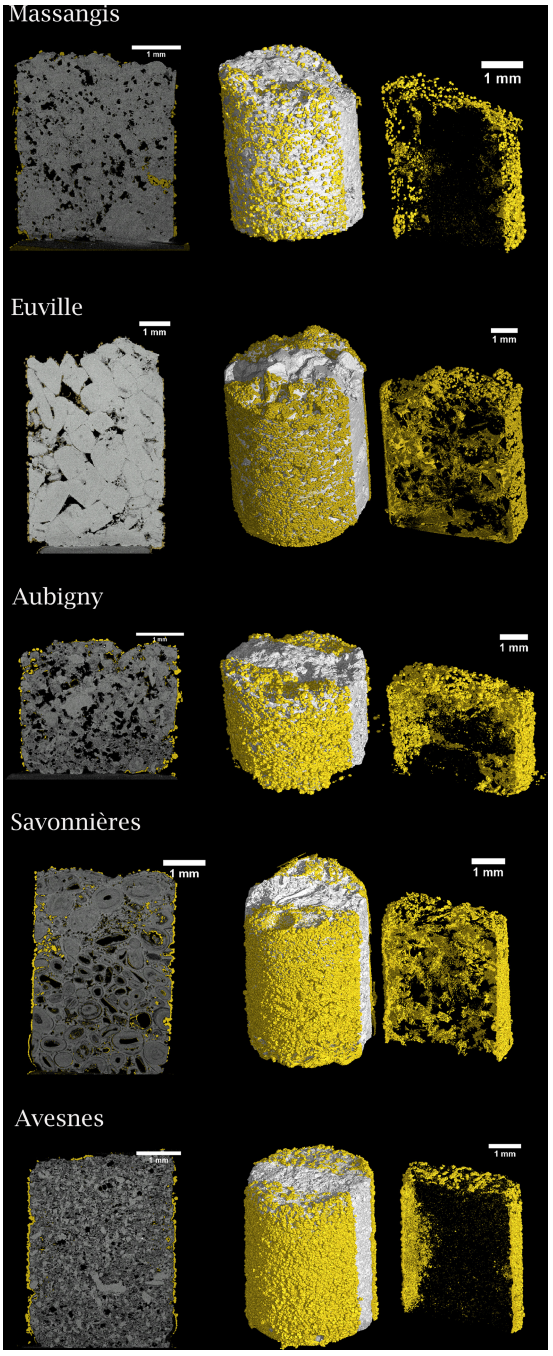

FIG. 5. 2D (left) and 3D (middle and right) microtomographs of biodeposition-treated limestone. Limestone cylinders were treated on all sides by immersion. Newly formed carbonate crystals are yellow. A rectangular region (right picture) was extracted from the limestone core (middle picture) in order to get an appreciation of the distribution of the biogenic crystals inside the pores of the limestone. Note the differences in coverage and penetration depth in the different types of biodeposition-treated stone.

ferences were observed not only between crystals precipitated on different types of stone but also between crystals precipitated on different specimens of a certain type of stone. Despite this variation in size and morphology, all of the stone types exhibited the presence of biodeposited rhombohedral crystals. Imprints of bacterial cells were observed only in crystals on the surfaces of biodeposition-treated prisms (pictures not shown). Furthermore, large differences in the penetration depth and degree of coverage with biogenic crystals were observed between the biodeposition treatments applied to different types of stone (see Fig. 5), in which the smallest amounts of carbonate crystals and penetration depth (i.e., mainly on the surface) were observed in Massangis limestone (Fig. 4 and 5). Avesnes and Aubigny exhibited a dense layer of biogenic crystals on the outer surface of the stone, where precipitation occurred at greater depths (Fig. 5) than in Massangis, i.e., mainly between

300 and 500 μm. Euville and Savonnières, on the other hand, showed massive precipitation both on the surface and inside the pores of the stone (at depths of greater than 2 mm), the effect being most pronounced for Savonnières. EDX analyses confirmed that these newly formed crystals consisted of calcium carbonate. It should be noted, however, that the resolution of the microtomographic analyses in this study is about 4 μm (i.e., 0.1% of the diameter of the specimen). Therefore, clogging of pores with diameters of less than 4 μm could not be visualized, making it difficult to estimate the exact penetration depth of the biodeposition treatment on stones such as Massangis and Avesnes, where most of the pores are smaller than 4 μm.

(ii) Weight increase through biodeposition. The biodeposition treatment resulted in a weight gain of all stones, the effect being more pronounced in the more porous stones (Table 1). In the least (Massangis) and most (Avesnes) porous stones, absolute (relative) weight gains of about 0.27 g (1.49%) and 0.61 g (4.34%) were observed, respectively. The greatest weight gain, however, was observed in Savonnières, i.e., 0.65 g (4.51%).

Similar observations were made with the control series, in which the more porous stones exhibited, in general, a greater weight increase. In all of the control series, Massangis exhibited a significantly smaller weight increase than the other types of stone. The amount of bacterial culture liquid absorbed by Savonnières and Avesnes was more than twice that absorbed by Massangis. Similarly, the greatest weight increase due to the nutrients and calcium salts (i.e., medium series) was observed in Avesnes, i.e., about twice as great as that of Aubigny and Euville and three times as great as that of Massangis. In the supernatant series, Avesnes exhibited a weight increase three times that of Massangis.

(iii) Spectrophotometric analyses. Biodeposition-treated stones exhibited lower L^* values than the untreated samples, indicating a darkening of the surface. Furthermore, biodeposition-treated samples showed larger a^* and b^* values, indicating a shift toward red and yellow. Although significant differences between the b^* values of the different types of untreated limestone were observed, all biodeposition-treated limestones showed similar b^* values between 16 and 17.5. The overall degree of color change (expressed as ΔE values) was observed to be dependent on the type of stone; however, no relationship between the degree of color change and the amount of carbonate precipitated was found. The highest ΔE value, i.e., 14.6 (Table 2), was observed in the slightly porous limestone Massangis, in which the least biogenic carbonate was found (Table 1). On the contrary, a much smaller ΔE value, i.e., 7.9, was obtained for the highly porous Avesnes limestone, on which a large amount of biogenic carbonate was found (Table 1).

Evaluation of the protective performance of the biodeposition treatment. (i) Capillary water absorption. The biodeposition treatment resulted in a decreased rate of water uptake by all of the stones under investigation (Fig. 6A and B). The largest decrease was observed in Savonnières. In this type of stone, a 20× decreased rate of water absorption was observed after biodeposition treatment, and for the other types of stone, the decreases in water absorption rate were about 2× (Euville) to 7× (Aubigny). Biodeposition-treated Euville, Aubigny, and Avesnes stones exhibited somewhat lower final water absorption values than untreated stones.

TABLE 2. Influence of biodeposition treatment on the visual aspect of different types of stone[a]

Stone and treatment	L^*	a^*	b^*	ΔE^*
Massangis				
None	75.5 ± 2.1	2.0 ± 0.6	9.1 ± 1.2	
Biodeposition	62.8 ± 1.2	4.4 ± 0.4	16.0 ± 1.1	14.6 ± 1.6
Aubigny				
None	75.6 ± 3.0	3.5 ± 0.7	12.5 ± 1.4	
Biodeposition	64.7 ± 1.8	5.7 ± 0.5	18.1 ± 0.8	12.4 ± 2.2
Euville				
None	78.3 ± 1.0	2.6 ± 0.2	10.6 ± 0.9	
Biodeposition	69.7 ± 1.3	4.6 ± 0.5	16.3 ± 0.7	7.3 ± 1.0
Savonnières				
None	78.3 ± 2.2	2.1 ± 0.4	11.5 ± 0.7	
Biodeposition	66.4 ± 1.6	4.3 ± 0.3	16.5 ± 1.1	13.1 ± 1.8
Avesnes				
None	77.5 ± 1.9	1.7 ± 0.6	14.8 ± 1.2	
Biodeposition	70.2 ± 2.5	2.5 ± 0.6	17.5 ± 2.3	7.9 ± 2.1

[a] A decrease in the L^* value indicates a darkening of the surface. Increases in the a^* and b^* values correspond to shifts toward red and yellow, respectively. Values are means ± the standard errors of the means.

(ii) Drying behavior. The biodeposition treatment gave rise to a decreased rate of drying, with the effect being more pronounced for the more porous stones (Fig. 6C and D). The largest difference in drying behavior between untreated and biodeposition-treated stones was observed in the most porous stones, i.e., Avesnes and Savonnières, and for the least porous stone, i.e., Massangis, no difference in drying behavior between untreated and biodeposition-treated stones was observed.

(iii) Resistance to sonication. Biodeposition-treated stones showed about 50% less weight loss upon sonication than untreated stones (Fig. 7); furthermore, the weight loss was much smaller than the weight gain due to the biodeposition treatment (Table 1). Stones treated with medium (growth and biodeposition medium) or with supernatant exhibited a greater weight loss than the untreated stones, while the opposite was true for stones treated with bacteria. Figure 7 clearly shows the differences in cohesion between the different types of stone, in that the more porous stone, in general, exhibited greater weight loss upon sonication. In the most porous stone, i.e., Avesnes, a weight loss of about 1.4% (0.19 g) was observed, and in the least porous stone, i.e., Massangis, the weight loss amounted to about 0.2% (0.10 g).

(iv) Resistance to salt attack. The biodeposition treatment resulted in an increased resistance of stone to salt attack, with the effect being more pronounced for the more porous stones (Fig. 8). While biodeposition-treated Savonnières remained largely unaffected after 15 cycles of exposure to sodium sulfate, untreated stones were heavily degraded. No differences were observed in the resistance to salt attack of biodeposition-treated and untreated Massangis, in which only limited degradation was observed after 20 cycles of salt attack.

(v) Resistance to freezing and thawing. Biodeposition-treated stones exhibited a higher resistance to freezing and

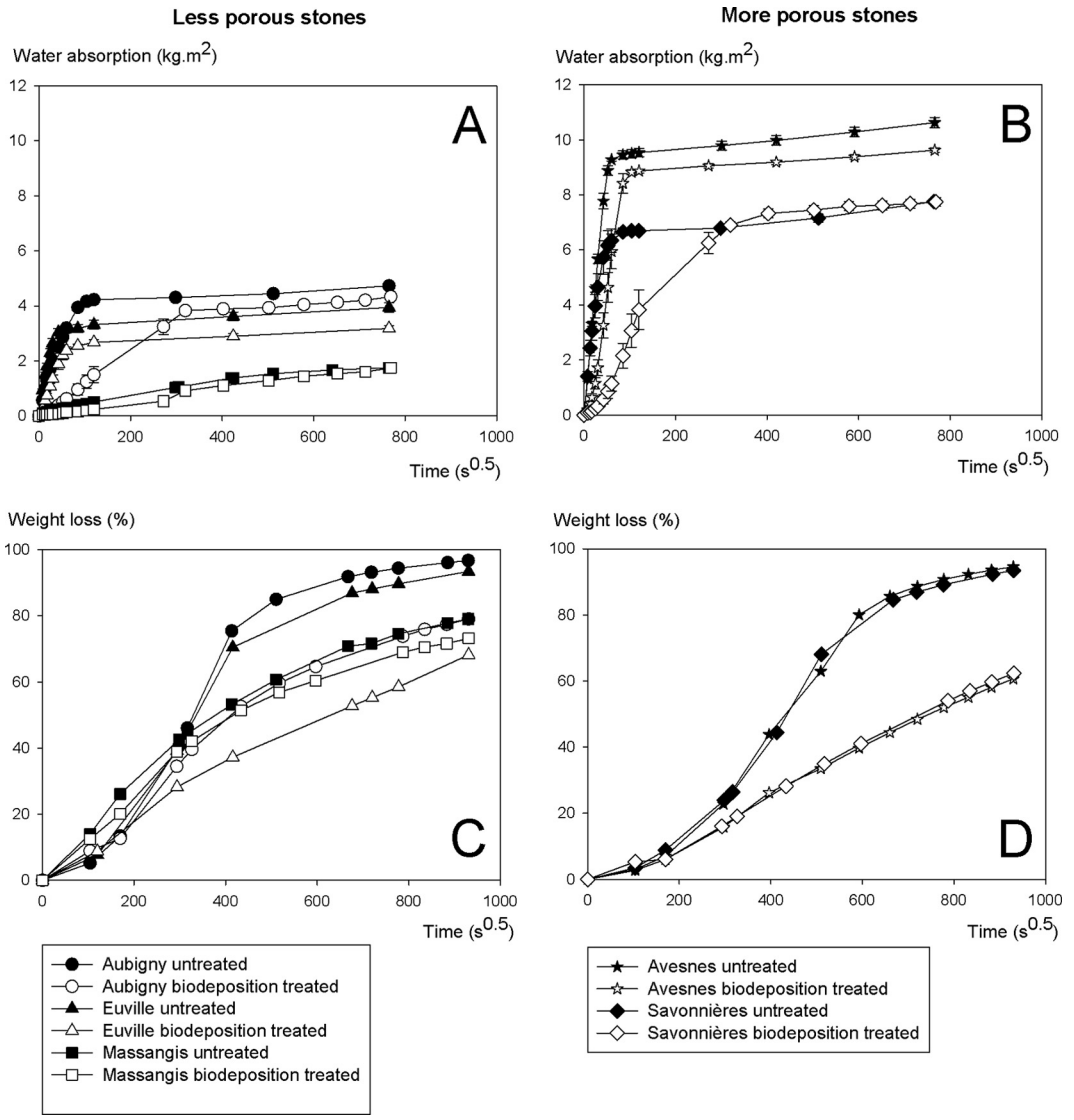

FIG. 6. Influence of the biodeposition treatment on the water absorption (A and B) and drying behavior (C and D) of stones that differ in porosity. Drying behavior is expressed as percent weight loss, i.e., the weight of the water lost due to evaporation compared to the weight of the water initially present inside the water-saturated stone.

thawing than untreated stones; the effect was most pronounced for Savonnières limestone (Fig. 9). After 14 cycles of freezing and thawing, untreated Savonnières was heavily degraded, while the biodeposition-treated stones remained largely unaffected. For the other types of stone, the differences in resistance to freezing and thawing were less pronounced, since only limited degradation was observed in the untreated stones (e.g., Massangis).

DISCUSSION

Characterization of the stone. Large differences in pore size distribution and porosity between the different types of stone were observed. Furthermore, for a given stone, different pore size distributions were obtained when using MIP or microtomography (Fig. 1), though more specifically, MIP underestimated the amount of macropores. This can be attributed to the ink bottle effect and/or the fact that some of these macropores (air voids) are not connected to the pore network or surface and hence cannot be penetrated by water or mercury. The ink bottle effect occurred for large pores that are connected to the surface by small pores. During intrusion measurements, mercury is able to enter these large pores only at the higher breakthrough pressures associated with the small connecting pores. The latter made it difficult to determine the presence of large pores, since MIP measures the radii of the connecting pores (19). Since absorption of bacteria occurs mainly in surface macropores (see below), MIP gave a good estimation of the amount of macropores accessible to bacteria.

Characterization of the urease activity inside the stone. Different types of limestone exhibited different urease activities upon transfer from a *B. sphaericus* culture to a urea-containing solution (Fig. 2C). The urease activities measured inside the stones (0.02 to 0.12 mM urea min^{-1}) were lower than the urease activities of the 1-day-old cultures (1 and 0.26 mM urea

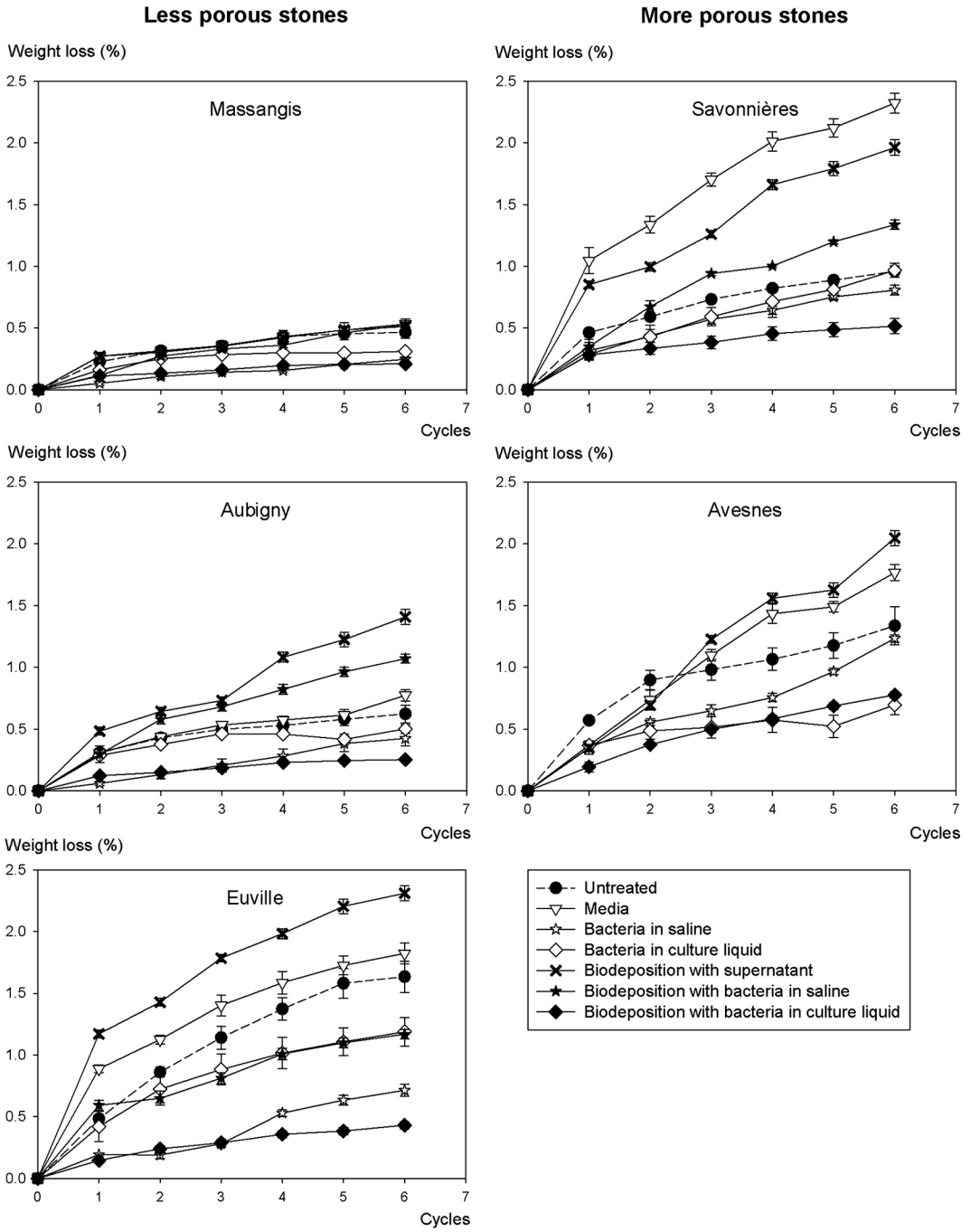

FIG. 7. Influence of the biodeposition treatment on the resistance of stone to sonication. The lower the weight loss after sonication, the greater the consolidating effect of the treatment.

min^{-1} in the absence and presence of calcium, respectively). Differences in urease activity between the different types of stone may be attributed to differences in the number of cells present in the stone (Fig. 2A). From the findings shown in Fig. 2, it appears that at least 10^9 cells were present inside or on the stone. Besides differences in cell numbers, the lower urea hydrolysis rates measured inside the stones than in the starting cultures were attributed to the slow diffusion of nutrients inside the stone.

The urease activity of the 1-day-old cultures falls within the range of urease activities required for biocementation purposes (0.5 to 50 mM urea min^{-1}) (18), although situated in the lower range; however, in studies on sand consolidation, it was found that lower urea hydrolysis rates resulted in greater strength improvement. During the exponential growth phase, *B. sphaericus* cultures exhibited a specific urease activity of about 10 mM urea min^{-1}, which is in the range of the values observed for *Sporosarcina pasteurii* in studies on biocementation (30, 31).

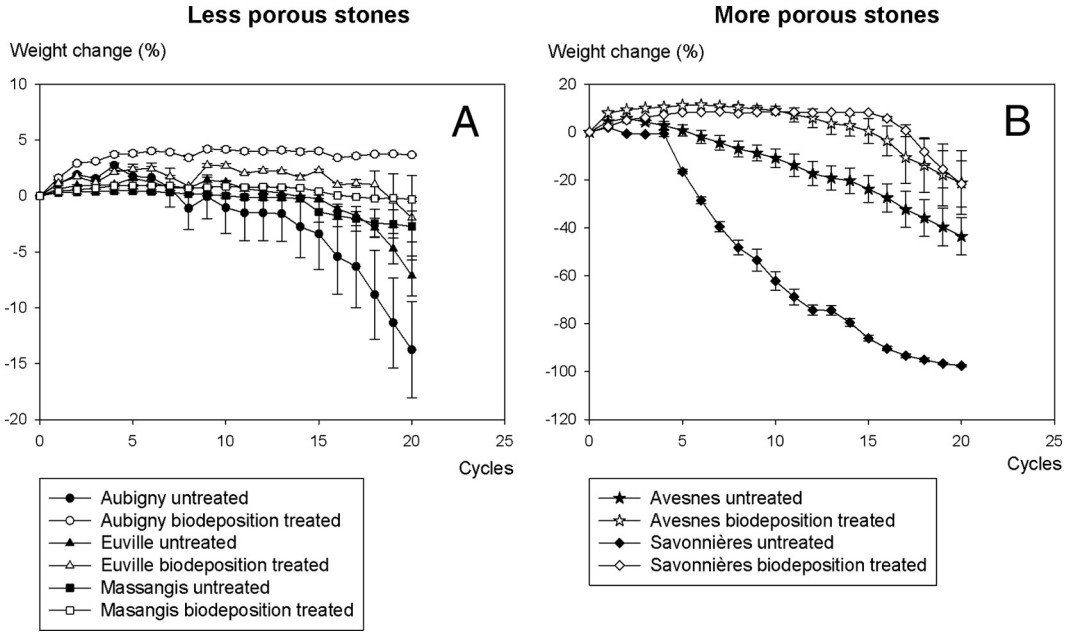

FIG. 8. Influence of the biodeposition treatment on the resistance of stone to salt attack. A smaller weight loss after freezing and thawing indicates higher resistance to salt attack. Note the difference in scale between the *y* axes of the two graphs. Weight loss is expressed as a percentage of the initial dry weight of the stone.

In the presence of calcium ions, the amount of urea hydrolyzed rapidly decreased with decreasing cell numbers (Fig. 2B), which can be attributed to the detrimental effect of the precipitation on the bacterial activity, i.e., formation of a diffusion barrier around the cell (31). The latter limits the access to nutrients and the removal of by-products. Additionally, entrapment of cells inside calcareous flocks results in a decrease in the number of active cells (30). With increasing numbers of bacteria initially present, a higher rate of survival, and hence ureolytic activity, can be expected.

Characterization of the biodeposition layer. The production and distribution of biogenic crystals were influenced by the pore structure of the stone and the biodeposition treatment procedure. The fact that experiments were performed by immersion in stagnant water had two important consequences. (i) Transport of urea, carbonate, and calcium ions was mainly diffusion controlled, and (ii) precipitation of calcium carbonate was not restricted to the volume of the stone but could also occur in the bulk solution.

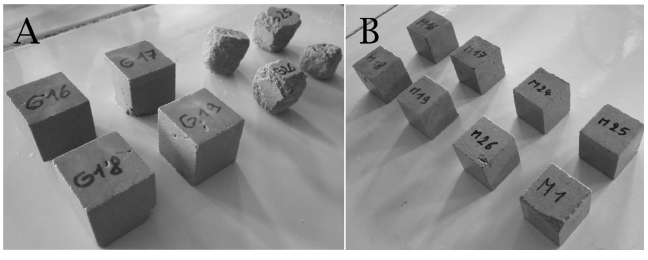

FIG. 9. Visual appearance of Savonnières (A) and Massangis (B) limestone cubes after 14 cycles of freezing and thawing. The four cubes on the left were biodeposition treated, while the four cubes on the right were untreated.

From Table 1, it follows that for the different types of stone, the presence of nutrients and calcium salts (medium series) and that of bacterial culture liquid (bacteria in culture liquid series) maximally account for 36% and 13% of the weight increase due to biodeposition treatment, respectively. Therefore, the overall weight increase after a biodeposition treatment can be attributed mainly to the precipitation of calcium carbonate.

Initial precipitation occurred on the outer surface of the stone, i.e., the interface where opposing gradients of carbonate and calcium met. Carbonate ions present inside the stone (originating from hydrolyzed urea in the bacterial culture solution) migrated outward and reacted with calcium ions from the biodeposition medium that diffused inside the stone. Precipitation occurred when the pore or bulk solution was locally supersaturated with calcium and carbonate ions. Since this initial precipitation depends on both diffusion and the amount of carbonate present, its extent was governed mainly by the pore structure of the stone, which was clearly shown by the weight gain of stones treated with the bacterial culture supernatant (Table 1), i.e., series where no secondary precipitation occurred (see below). The greater weight gain observed in more porous stones can be attributed to the larger amount of carbonate absorbed after 1 day of immersion in the supernatant. Upon transfer to the biodeposition medium, this resulted in greater production of biogenic crystals. The lower weight gain observed in Euville and Savonnières than in Aubigny and Avesnes, respectively, can be attributed to the relatively larger amount of macropores in the former. Upon transfer to the biodeposition medium, carbonate ions present inside surface macropores were more rapidly leached to the bulk solution than were carbonate ions present in micropores (see the section on resistance to sonication below). Greater leaching im-

plies less carbonate precipitation in/on the stone and hence a lower weight gain. For the current biodeposition procedure, i.e., biodeposition with bacteria in culture liquid, initial precipitation accounts for maximally 30 to 50% of the overall weight increase (supernatant series in Table 1).

Gradually, precipitation from urea hydrolyzed *in situ* also occurred. Since this secondary precipitation depends on the presence of bacteria, its location was dependent on the pore structure of the stone. Samonin and Elikova (22) reported that for maximum absorption of microbial cells, the absorbent pores must be two to five times larger than the cells. Since cells of *B. sphaericus* have dimensions of about 1 to 4 μm, bacteria are absorbed mainly by surface pores with diameters larger than 2 μm (further indicated as macropores). The latter explains why in Savonnières (i.e., macroporous stone), precipitation was clearly observed throughout the stone, while in Massangis (microporous stone), precipitation was restricted mainly to the outer surface (Fig. 5). Furthermore, the larger amount of macropores in Savonnières than in the other stones explains the greater weight gain observed after the biodeposition treatment with bacteria in saline (Table 1). This can be attributed to the fact that more bacteria were retained in Savonnières and to the fact that hydrolysis of urea in the presence of calcium increases with an increasing number of bacteria (Fig. 2B). Leaching of bacteria from the stone to the biodeposition medium was limited due to flocculation of the cells inside the pores in the presence of calcium ions (14, 27).

The observed variations in crystal size and morphology may be attributed to differences in local urease activity during the initial and secondary precipitations. Smaller crystals arose in areas where fast supersaturation occurred, such as on the surface and inside macropores, i.e., areas with high ureolytic activity and/or more rapid diffusion of reactants. Rhombohedral crystals, characteristic of calcite, were observed on all types of stone. The imprints of bacterial cells indicate microbial involvement in the carbonate precipitation seen.

The absorption of bacteria in (macro)pores and an improved penetration depth may be beneficial for applications in practice. This absorption may protect bacteria from desiccation or washing out by rainfall and hence failure of the biodeposition treatment. Therefore, it seems that biodeposition will be more feasible on macroporous stone than on microporous stone, where bacteria are adsorbed only on the outer surface.

The biodeposition treatment resulted in a change in the visual aspect of the surface of the different types of limestone (Table 2). The ΔE values observed in this research, however, are rather high, especially since ΔE values below 5 (23) or 6 (29) are generally considered to be acceptable for surface treatments on stone. As indicated in our previous study (9), these high ΔE values can be attributed mainly to the presence of yeast extract (orange in color when a powder) in the growth medium. We are currently investigating alternative growth media in order to decrease the change in visual appearance resulting from the biodeposition treatment.

Evaluation of the protective performance of the biodeposition treatment. (i) Capillary water absorption. As indicated in our previous study, the decrease in water uptake observed in biodeposition-treated stones was attributed to the presence of biogenic carbonate crystals, since no decrease in water absorption was observed in control series without bacteria and/or a calcium source (9). Furthermore, it was observed that treatments which resulted in a larger amount of carbonate precipitation gave rise to a more pronounced decrease in water absorption. The presence of biogenic crystals resulted in blocking of the pores and/or decreased pore diameters. The fact that Savonnières exhibited the highest decrease in water uptake might be attributed to the larger amount of biogenic carbonate deposited in the pores and on the surface (Table 1 and Fig. 5). Despite the fact that Euville and Aubigny exhibited similar amounts of carbonate precipitation, a much greater decrease in water uptake was observed in the latter. This might be attributed to differences in pore size distribution, which not only governs the distribution of the biogenic carbonate but also affects the water absorption rate.

(ii) Drying behavior. The decreased rate of drying of biodeposition-treated stone can be attributed to blocking of the pores and decreased pore diameters near the surface resulting from the presence of biogenic crystals. As indicated earlier, more porous stones exhibited more biogenic crystal formation (Table 1); hence, the permeability and drying behavior of more porous stone were affected more by biodeposition than those of less porous stone, due to the larger amount of pores blocked or filled with carbonate crystals.

Despite the fact that biodeposition-treated stones showed a lower rate of drying than untreated stones, in practice, it can be expected that, in most cases, biodeposition-treated stones will contain less water than untreated stones due to their slower water uptake. The decreased rate of drying did not increase the risk of freeze-thaw damage (see below).

(iii) Resistance to sonication. Prisms treated with bacteria in culture liquid and biodeposition medium exhibited greater resistance to sonication (i.e., lower weight loss) than did untreated prisms (Fig. 7), indicating that the biogenic carbonate crystals were firmly attached to the surface and that they exerted a consolidating effect. This is in agreement with observations made by the research team of Rodriguez-Navarro et al. (16, 21) and previous work (9) in which the consolidating effect can be attributed to the formation or an extension of the cementing layer between two grains. With an increased contact area between two grains, there is a decreased chance of detachment upon sonication.

Prisms treated with the supernatant and the biodeposition medium exhibited greater weight loss than untreated prisms, indicating that biogenic carbonate crystals that were formed during initial precipitation, i.e., reaction between carbonate ions in the bacterial culture liquid and calcium ions from the biodeposition medium, did not adhere strongly to the surface and did not exert any consolidative effect. The greater weight loss in the nutrient series than in the control series can be attributed to leaching from the nutrients. The difference in weight loss between the former two series was much larger with Savonnières and Euville than with Avesnes and Aubigny, respectively, which can be attributed to the more rapid leaching from macropores, as indicated earlier. Despite their lower weight gain, biodeposition series treated with bacteria in saline exhibited greater weight losses after sonication than biodeposition series treated with bacteria in culture liquid. Differences in the adhesion of biogenic carbonates to stone between the two series may be attributed to the rate at which supersaturation, and hence precipitation, occurred. In their work on biode-

position, Rodriguez-Navarro et al. observed that low supersaturation values result in the formation of crystals that exhibit equilibrium morphology (rhombohedra) and that adhere better to stone (21). In our study, the presence of an ammonium-ammonia buffer system in the culture liquid prevented rapid pH variations and high supersaturation upon the hydrolysis of urea, while this was not the case for the prisms treated with bacteria in saline. The lower weight loss observed in the bacterial series than in the medium and supernatant series can be attributed to the lower weight gain of the former (Table 1). The fact that the bacterial series exhibited less weight loss than the untreated series may be attributed to the dissolution of calcium carbonate in the saline solution or culture liquid, as was observed from a shift in the pH of these solutions (Table 1). Therefore, a substantial part of the crystals that are normally removed during the first sonication cycle (i.e., the cycle in which the largest weight loss is observed) were already removed before the sonication tests, while this was not the case for the untreated specimens.

From the results described above, it follows that in order to increase the consolidative effect of the biodeposition treatment, one has to increase the *in situ* precipitation of $CaCO_3$ and to decrease the precipitation of calcium with carbonates from the bacterial culture liquid. The latter can be achieved by decreasing the amount of urea in the growth medium or using centrifuged cultures (which is less feasible for applications in practice). Exclusion of urea (and carbonates) from the growth medium is not possible for cultures of *B. sphaericus* LMG 22257 or *S. pasteurii* (30), since these organisms require urea or ammonium and alkaline pH values for growth.

(iv) Resistance to salt attack and freezing and thawing. The increased resistance of biodeposition-treated stone to salt attack, as observed in the testing procedure applied in this research, can be attributed to the decreased rate of water uptake, which implies that smaller amounts of salts are absorbed by biodeposition-treated stone than by untreated stone. Indeed, biodeposition-treated Savonnières, which showed the largest decrease in water absorption also exhibited the highest increase in resistance to salt attack. Additionally, the consolidating effect of the biogenic crystals, as observed from the sonication experiments, might have increased the resistance to damage resulting from crystallization pressure. Similarly, Aubigny, in which the biodeposition treatment resulted in a much larger decrease in water absorption than in Euville, exhibited a greater increase in resistance to salt attack after biodeposition treatment than Euville did. Like the salt attack resistance, the increased resistance to freezing and thawing can be attributed to the consolidative effect of the biodeposition treatment and decreased water absorption.

(v) General considerations and concluding remarks. The main focus of this research paper is the influence of pore structure on both the penetration depth and the efficiency of the biodeposition treatment. Pore structure affects the transport of bacteria and hence the amount and distribution of biogenic carbonate; however, in addition to pore structure, transport of bacteria depends on the adsorption of bacteria to the mineral matrix. As indicated earlier, adsorption of bacteria is governed by a variety of physical, chemical, and microbiological factors (25). All of the stone types under investigation consist mainly of carbonate. Therefore, it can be expected that differences in adsorption due to differences in physicochemical characteristics are not the main parameters affecting the amount of biogenic precipitation, especially since adsorption of bacteria is not a prerequisite for hydrolysis of urea to occur. Hydrolysis of urea also occurs from bacteria that are present inside the pores without being adsorbed to the pore walls, i.e., bacteria that are present in suspension or in flocks. The latter can be attributed to the presence of calcium ions in the biodeposition medium, which results in the flocculation of cells. Flock formation promotes the retention of bacteria inside the porous matrix (14). From the results described above, it can be concluded that pore structure, governing bacterial retention, is one of the main parameters affecting biodeposition.

In our studies thus far, biodeposition treatment was applied under controlled and optimal conditions, i.e., immersion at 28°C. In future research, the effectiveness of biodeposition treatment will be investigated when applied under conditions relevant to practice, i.e., spraying at lower temperatures. Attention will also be paid to the composition of the growth medium, since it has an enormous impact on the visual appearance of the stone after biodeposition treatment.

This was the first study in which the penetration of the biodeposition treatment in the stone was visualized. From the microtomographic analyses, it was clear that for Euville and Savonnières, penetration depths of greater than 2 mm were observed, which are much greater than the values reported previously for the different types of biodeposition treatment (between a few and hundred micrometers [see above]). For macroporous stones, it can be expected that even greater penetration depths can be obtained. Given that the effectiveness of a consolidant depends on its penetration depth, future research will focus on the optimization of the penetration depth of the biodeposition treatment. Greater penetration depths could be obtained, for instance, by using spores instead of living cells. Due to their smaller diameter, spores can be transported to greater depths and, upon germination, precipitate carbonate at greater depths. Due to its higher porosity, for Savonnières, even higher dosages of bacteria and nutrients may be applied to increase the effectiveness of the biodeposition treatment. Despite the fact that greater penetration depths were observed in Euville and Savonnières than in the other types of limestone (Massangis, Aubigny, and Avesnes), no differences in the consolidative effect of the biodeposition treatments applied to different types of stone were observed in sonication experiments. This might indicate that sonication experiments are not sensitive enough to evaluate the consolidative effect on quarry (i.e., nondegraded) stone at greater depths. Therefore, future experiments will be performed with degraded stone.

This study indicated that the largest biogenic carbonate production occurred in stones with a large amount of macropores (Savonnières), which is attributable to the fact that adsorption of bacterial cells (1 to 4 μm) is known to occur in pores with dimensions of 4 to 20 μm. The greater carbonate production and penetration depth account for the larger protective effect observed in more macroporous stones. The larger amount of biogenic carbonate crystals resulted in a greater decrease in water uptake and, as a consequence, greater resistance to water-related degradation processes, i.e., salt attack and freezing and thawing.

ACKNOWLEDGMENTS

Willem De Muynck works as a postdoctoral fellow of the Flemish Agency for Innovation by Science and Technology (Flanders, Belgium). Denis Van Loo is supported by the Fund for Scientific Research Flanders (project G.0100.08).

We thank Tom Hennebel, Kim Van Tittelboom, and Jan Dewanckele for critically reading the manuscript, Peter Mast for performing the SEM analyses, and Melissa Dunkle for proofreading.

REFERENCES

1. **Adolphe, J. P., J. F. Loubière, J. Paradas, and F. Soleilhavoup.** 1990. Procédé de traitement biologique d'une surface artificielle. European patent 90400G97.0.
2. **Berger-Schunn, A.** 1994. Practical colour measurement, a primer for the beginner, a reminder for the expert. Wiley, New York, NY.
3. **Castanier, S., G. Le Metayer-Levrel, and J.-P. Perthuisot.** 1999. Ca-carbonates precipitation and limestone genesis—the microbiogeologist point of view. Sediment. Geol. **126:**9–23.
4. **Cnudde, V., J. P. Cnudde, C. Dupuis, and P. J. S. Jacobs.** 2004. X-ray micro-CT used for the localization of water repellents and consolidants inside natural building stones. Mater. Charact. **53:**259–271.
5. **De Muynck, W.** 2009. Microbial interactions with mineral building materials. Ph.D. dissertation. Ghent University, Ghent, Belgium.
6. **De Muynck, W., K. Cox, N. De Belle, and W. Verstraete.** 2008. Bacterial carbonate precipitation as an alternative surface treatment for concrete. Constr. Build. Mater. **22:**875–885.
7. **De Muynck, W., N. De Belie, and W. Verstraete.** 2010. Microbial carbonate precipitation in construction materials: a review. Ecol. Eng. **36:**118–136.
8. **De Muynck, W., D. Debrouwer, N. De Belie, and W. Verstraete.** 2008. Bacterial carbonate precipitation improves the durability of cementitious materials. Cem. Concr. Res. **38:**1005–1014.
9. **De Muynck, W., K. Verbeken, N. De Belie, and W. Verstraete.** 2010. Influence of urea and calcium dosage on the effectiveness of bacterially induced carbonate precipitation on limestone. Ecol. Eng. **36:**99–111.
10. **Dick, J., et al.** 2006. Bio-deposition of a calcium carbonate layer on degraded limestone by Bacillus species. Biodegradation **17:**357–367.
11. **Hammes, F., N. Boon, J. de Villiers, W. Verstraete, and S. D. Siciliano.** 2003. Strain-specific ureolytic microbial calcium carbonate precipitation. Appl. Environ. Microbiol. **69:**4901–4909.
12. **Hammes, F., A. Seka, S. de Knijf, and W. Verstraete.** 2003. A novel approach to calcium removal from calcium-rich industrial wastewater. Water Res. **37:**699–704.
13. **Hammes, F., and W. Verstraete.** 2002. Key roles of pH and calcium metabolism in microbial carbonate precipitation. Rev. Environ. Sci. Biotechnol. **1:**3–7.
14. **Harkes, M. P., L. A. van Paassen, J. L. Booster, V. S. Whiffin, and M. C. M. van Loosdrecht.** 2010. Fixation and distribution of bacterial activity in sand to induce carbonate precipitation for ground reinforcement. Ecol. Eng. **36:** 112–117.
15. **Jakobsen, U. H., and D. R. Brown.** 2006. Reproducibility of w/c ratio determination from fluorescent impregnated thin sections. Cem. Concr. Res. **36:**1567–1573.
16. **Jimenez-Lopez, C., et al.** 2007. Consolidation of degraded ornamental porous limestone stone by calcium carbonate precipitation induced by the microbiota inhabiting the stone. Chemosphere **68:**1929–1936.
17. **Karatasios, I., P. Theoulakis, A. Kalagri, A. Sapalidis, and V. Kilikoglou.** 2009. Evaluation of consolidation treatments of marly limestones used in archaeological monuments. Constr. Build. Mater. **23:**2803–2812.
18. **Kucharski, E. S., R. Cord-Ruwisch, V. Whiffin, and S. M. J. Al-Thawadi.** 2006. Microbial biocementation. World patent 066326.
19. **Leith, S. D., M. M. Reddy, W. F. Ramirez, and M. J. Heymans.** 1996. Limestone characterization to model damage from acidic precipitation: effect of pore structure on mass transfer. Environ. Sci. Technol. **30:**2202–2210.
20. **Le Metayer-Levrel, G., S. Castanier, G. Orial, J. F. Loubiere, and J. P. Perthuisot.** 1999. Applications of bacterial carbonatogenesis to the protection and regeneration of limestones in buildings and historic patrimony. Sediment. Geol. **126:**25–34.
21. **Rodriguez-Navarro, C., M. Rodriguez-Gallego, K. Ben Chekroun, and M. T. Gonzalez-Munoz.** 2003. Conservation of ornamental stone by *Myxococcus xanthus*-induced carbonate biomineralization. Appl. Environ. Microbiol. **69:** 2182–2193.
22. **Samonin, V. V., and E. E. Elikova.** 2004. A study on the absorption of bacterial cells on porous materials. Microbiology **73:**696–701.
23. **Sasse, H. R., and R. Snethlage.** 1996. Evaluation of stone consolidation treatments. Sci. Technol. Cult. Herit. **5:**85–92.
24. **Stevik, K. T., A. Kari, G. Ausland, and F. J. Hanssen.** 2004. Retention and removal of pathogenic bacteria in wastewater percolating through porous media: a review. Water Res. **38:**1355–1367.
25. **Torraca, G.** 1975. Treatment of stone in monuments. A review of principles and processes. International Symposium on Conservation of Stone I, Bologna, Italy.
26. **Vance, D. B.** 1995. Particulate transport in groundwater part II—bacteria. Nat. Environ. J. **5:**25–26.
27. **Van Paassen, L., V. S. Whiffin, and M. P. Harkes.** 2007. Immobilization of bacteria to a geological material. Stichting Geodelft/Deltares, patent WO2007069884A1.
28. **Vlassenbroeck, J., et al.** 2007. Software tools for quantification of X-ray microtomography at the UGCT. Nucl. Instrum. Methods Phys. Res. A **580:** 442–445.
29. **Wetenschappelijk en Technisch Centrum voor het Bouwbedrijf.** 2002. Waterwerende oppervlaktebehandeling (vervangt TV 140). Wetenschappelijk en Technisch Centrum voor het Bouwbedrijf, Brussels, Belgium.
30. **Whiffin, V. S.** 2004. Microbial CaCO3 precipitation for the production of biocement. Ph.D. dissertation. Murdoch University, Perth, Australia. http://library.murdoch.edu.au/adt/browse/view/adt-MU20041101.142604.
31. **Whiffin, V. S., L. van Paassen, and M. P. Harkes.** 2007. Microbial carbonate precipitation as a soil improvement technique. Geomicrobiol. J. **24:**417–423.
32. **Zamarreño, D. V., R. Inkpen, and E. May.** 2009. Carbonate crystals precipitated by freshwater bacteria and their use as a limestone consolidant. Appl. Environ. Microbiol. **75:**5981–5990.